electronics

Communication

UTD-PO Solutions for the Analysis of Multiple Diffraction by Trees and Buildings When Assuming Spherical-Wave Incidence

José-Víctor Rodríguez [1,*], María-Teresa Martínez-Inglés [2], Jose-Maria Molina Garcia-Pardo [1], Leandro Juan-Llácer [1] and Ignacio Rodríguez-Rodríguez [3]

[1] Departamento de Tecnologías de la Información y las Comunicaciones, Universidad Politécnica de Cartagena, Antiguo Cuartel de Antigones, Plaza del Hospital 1, 30202 Cartagena, Spain
[2] Ministerio de Defensa-Universidad Politécnica de Cartagena, Departamento de Ingeniería y Técnicas Aplicadas, Centro Universitario de la Defensa, San Javier Air Force Base, 30720 Santiago de la Ribera, Spain
[3] Departamento de Ingeniería de Comunicaciones, Universidad de Málaga, Avda. Cervantes 2, 29071 Málaga, Spain
* Correspondence: jvictor.rodriguez@upct.es; Tel.: +34-968-326-548

Abstract: This paper presents two uniform theories of diffraction–physical optics (UTD-PO) formulations to undertake analysis of radiowave multiple diffraction resulting from the presence of both buildings and trees in vegetated urban areas, with the assumption of spherical-wave incidence. The solutions presented consider buildings modeled as knife-edges and rectangular sections (the latter being more complex and realistic) and the effect of the tree canopy (the assumption is that this exceeds the height of the average rooftop) is taken into account by adding proper attenuation factors/phasors to building diffraction phenomena. The validation of these formulations has been undertaken by comparing with other methods and measurements performed at 39 GHz on a scaled-model of the environment under analysis, consisting of an array of bricks and bonsai trees. The chief advantage of the solutions put forward is that because of recursion, the calculations only include single diffractions. This avoids any requirement for higher-order diffraction terms in the diffraction coefficients, which means less computer time/power is demanded. The results of this work may be useful when planning future mobile communication systems, including 6G networks and beyond.

Keywords: mobile communication; multiple diffraction; uniform theory of diffraction; vegetation

Citation: Rodríguez, J.-V.; Martínez-Inglés, M.-T.; Garcia-Pardo, J.-M.M.; Juan-Llácer, L.; Rodríguez-Rodríguez, I. UTD-PO Solutions for the Analysis of Multiple Diffraction by Trees and Buildings When Assuming Spherical-Wave Incidence. *Electronics* **2023**, *12*, 899. https://doi.org/10.3390/electronics12040899

Academic Editors: Minhoe Kim, Ohyun Jo and Byungchang Chung

Received: 19 January 2023
Revised: 8 February 2023
Accepted: 9 February 2023
Published: 10 February 2023

1. Introduction

When studying the propagation of radio waves in urban/semi-urban scenarios, we must accept the need to analyze the multiple diffraction phenomenon experienced by waves as they come into contact with the roofs of buildings, as it is one of the chief three attenuation factors existing within these environments (the other two being free-space losses and attenuation caused by ultimate diffraction to street-level) [1]. With regard to this, many different formulations have been put forward, with their basis in either physical optics [2,3] or the Uniform Theory of Diffraction (UTD) [4,5]. On the other hand, radio wave multiple diffraction caused by the presence of a series of trees has been widely analyzed in such works as [6–10]. Nevertheless, in undertaking analysis of vegetated residential environments, this multiple-diffraction analysis must incorporate the influence of trees located around buildings (which cause their own particular attenuation because of the canopy leaves).

In this sense, previous solutions that account for the analysis of the mentioned scenario have been proposed for both UHF [11–13] and millimeter-wave frequencies [14]. However, such formulations assume a plane-wave incidence over the array of obstacles and, when we take into account that, particularly with micro- or pico-cellular systems, transmitting antennas may be positioned very close to the series of obstacles, it could be more appropriate to make an assumption of spherical-wave incidence in order to achieve more accuracy and realism in predictions for multiple-diffraction attenuation.

This research presents two UTD-PO formulations to estimate the multiple-diffraction attenuation that occurs in vegetated residential environments where both buildings and trees are present, with the assumption of spherical-wave incidence. One solution assumes that buildings are shaped as knife edges, and this is then expanded to consider buildings shaped in rectangular sections (which has greater realism and provides more accuracy in outcomes); this gives the second solution that this research puts forward. The main advantage of the two formulations offered is that because of recursivity, the calculations for all iterations require only single diffractions. Thus, we avoid requirements for the diffraction coefficients to contain higher-order diffraction terms, which reduces the amount of computer time/power demanded. The multiple-diffraction attenuation results obtained theoretically are properly compared to those derived from a measurement campaign at 39 GHz undertaken on a scaled-model of the environment under analysis, made of bricks and bonsai trees. It is important to note that all empirical results put forward in this research are derived from laboratory experimentation. In this sense, as [15] illustrates, having measurements derived from laboratory studies—involving either scale or actual size models—has the advantage that they have been undertaken within controlled environments, allowing for every parameter to be accounted for, whilst simultaneously offering information that can be usefully employed in real-world radio propagation scenarios.

2. Propagation Environment

Figure 1 (top) illustrates the propagation scenario under consideration in this research, showing a group of n buildings of equal height, with trees next to them.

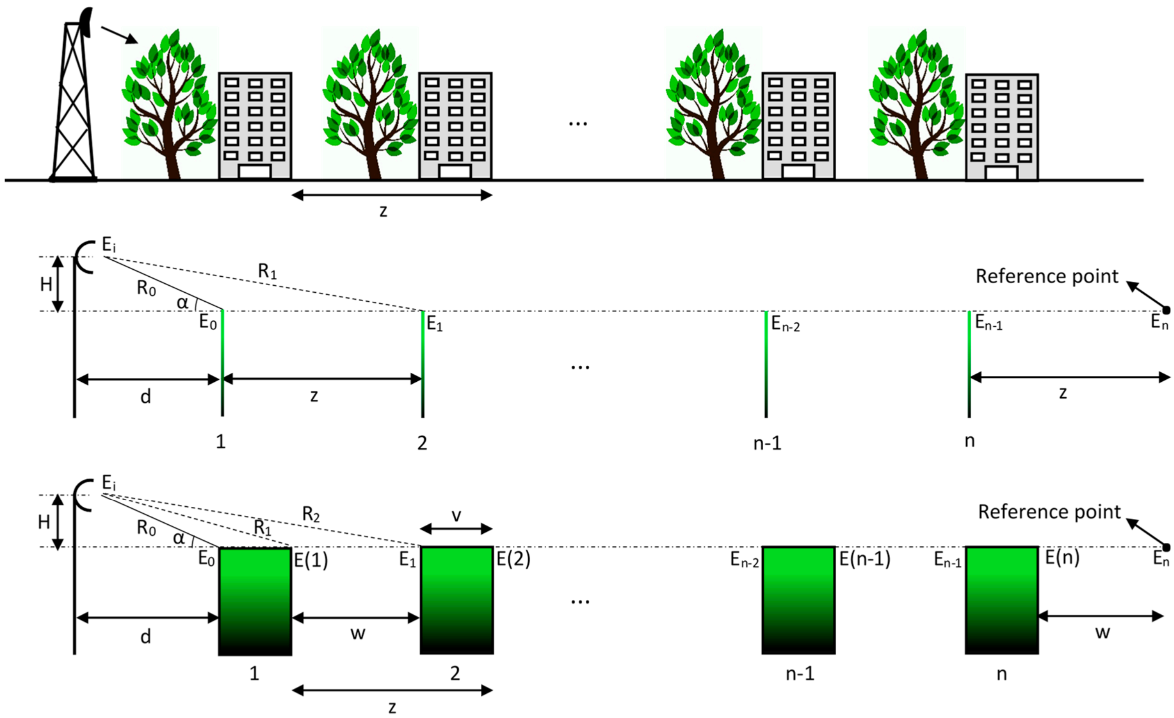

Figure 1. Propagation scenario under consideration for vegetated residential areas having trees and buildings in rows (**top**), and the same environment with buildings shaped as knife edge forms (**middle**) and as rectangular sections (**bottom**).

It is assumed that the space z between each pair of trees and buildings is constant and that the tree canopy exceeds the average height of the building. This means that the direct ray (LOS path) for the spherical wave that impinges with the positive incident angle α across the group of obstacles encounters obstruction from the tree canopies (as also occurs with the diffracted rays). The middle illustration of Figure 1 shows a theoretical propagation scenario whereby every pair of buildings/trees has undergone replacement with an absorbing knife edge (illustrated in black and green). This type of knife edge (with the spacing z still being constant) incorporates the influence of the tree canopy and the buildings in terms of the diffraction phenomenon encountered by waves, which leads to the initial theoretical formulation that will be detailed in the following section. Furthermore, the transmitting antenna, having a height H in relation to the height of the average building, has a location at a set distance d from the obstacle array, which means they are impinged by a spherical wave. In order that the buildings could be more realistically modeled, the bottom of Figure 1 shows an environment in which every pair of buildings and trees has undergone replacement with a finitely conducting block (rectangular section), pictured in black and green, with the width v. In this instance, the assumption is made that the rectangles have a constant spacing of w so that v + w = z; they also include the influence of buildings/tree canopies with respect to the diffraction phenomena, from which we derive the second theoretical formulation that will then be presented.

3. Theoretical Formulations

Through consideration of the two-dimensional (2D) UTD-PO solutions for analyzing multiple-diffraction of spherical waves by rows of knife edges and rectangular sections previously published by some of the researchers involved in this work in [16], in this paper, new theoretical formulations that include the influence of the tree canopies are presented. They have been developed by multiplying, where appropriate, an attenuation factor and corresponding phase factors by both diffracted and direct terms so that the influence of the tree canopies have joint consideration with the other obstacles.

3.1. Buildings Modeled as Knife-Edges

As stated before, by considering the UTD-PO formulation presented in [16] for the analysis of the multiple diffraction caused by an array of knife-edges—when assuming spherical-wave incidence—we may calculate the total field that reaches the reference point shown in Figure 1 (middle) with the following formula, where recursion allows for the field to be expressed in terms of single diffractions, thereby providing a straightforward and fast calculation that does not need to incorporate higher-order diffraction terms:

For $n \geq 1$,

$$\begin{aligned} E_n = \frac{1}{n}\Big[& E_0 A \Big[\frac{R_0}{R_n}\exp(-jk(R_n - R_0))\exp(-j\Delta k \Delta d\cos\alpha) + \sqrt{\frac{R_0}{nw[R_0+nz]}} \\ & \cdot D\Big(\phi = \frac{3\pi}{2}, \phi' = \frac{\pi}{2}+\alpha, L = \frac{R_0 nz}{R_0+nz}\Big)\exp(-jknz)\exp(-j\Delta k\Delta d)\Big] \\ & + \sum_{m=1}^{n-1} E_m\Big[\frac{R_0}{R_{n-m}}\exp(-jk(R_n - R_m)) + \sqrt{\frac{R_0}{(n-m)z[R_0+(n-m)z]}} \\ & \cdot D\Big(\phi = \frac{3\pi}{2}, \phi' = \frac{\pi}{2}+\alpha, L = \frac{R_0(n-m)z}{R_0+(n-m)z}\Big)\exp(-jk(n-m)z)\Big]\Big] \end{aligned} \tag{1}$$

where

$$R_x = \sqrt{H^2 + (d + x\cdot z)^2} \tag{2}$$

$$E_0 = \frac{E_i}{R_0}\exp(-jkR_0) \tag{3}$$

where E_i represents the relative amplitude of the spherical source and k represents the wavenumber, $D(\phi, \phi', L)$ provides the UTD diffraction coefficient when an absorbing knife-edge is used, as shown in [17], where Δd represents average propagation path length moving through the tree canopy,

$$A = \exp\Big(-\frac{L_v}{8.686}\Big) \tag{4}$$

and L_v represents the attenuation (in dB) caused by vegetation (relative to free space); therefore

$$L_v = \begin{cases} 26.6 f^{-0.2} \Delta d^{0.5} \text{ trees out} - \text{of} - \text{ leaf} \\ 15.6 f^{-0.009} \Delta d^{0.26} \text{ trees in} - \text{leaf} \end{cases} \tag{5}$$

with the assumption of the COST235 model [18], showing f in MHz and Δd in m,

$$\Delta k = k(n_R - 1) \tag{6}$$

with n_R representing the real part of the leaves' refractive index [19]

$$n_R = \sqrt{\varepsilon' + n_I^2} \tag{7}$$

and n_I is the imaginary part of the leaves' refractive index

$$n_I = \frac{L_v}{8.686} \text{ when } \Delta d = 1 \text{ m} \tag{8}$$

with ε' being the real part of the leaves' relative permittivity

$$\varepsilon' = A' - B' m_d \tag{9}$$

with

$$0.1 \leq m_d \leq 0.5 \tag{10}$$

Coefficient values for A' and B' are shown in [19]. In this research, typical values of m_d = 0.3, A'= 8.8 and B' = 4.3 are used.

3.2. Buildings Modeled as Rectangular Sections

Employing identical methods as Section 3.1, and considering the UTD-PO formulation presented in [16] for the analysis of multiple diffraction caused by a series of rectangular sections—when assuming spherical-wave incidence—we can calculate the total field reaching the reference point shown in Figure 1 (bottom); thus (again, recursion allows for the field to be expressed in terms of single diffractions):

For $n \geq 1$,

$$\begin{aligned} E_n = \frac{1}{2n} \Big\{ & E_0 A \Big[\frac{R_0}{R_{2n}} \exp[-jk(R_{2n} - R_0)] \exp(-j\Delta k \Delta d \cos\alpha) + \sqrt{\frac{R_0}{n(v+w)[R_0 + n(v+w)]}} \\ & \cdot D\Big(\phi' = \frac{\pi}{2} + \alpha, \phi = \frac{3\pi}{2}, L = \sqrt{\frac{R_0 n(v+w)}{R_0 + n(v+w)}}\Big) \exp[-jkn(v+w)] \exp(-j\Delta k \Delta d) \Big] \\ & + \sum_{q=1}^{n-1} E_q \Big[\frac{R_0}{R_{2(n-q)}} \exp[-jk(R_{2n} - R_{2q})] + \sqrt{\frac{R_0}{(n-q)(v+w)[R_0 + (n-q)(v+w)]}} \\ & \cdot D\Big(\phi' = \frac{\pi}{2} + \alpha, \phi = \frac{3\pi}{2}, L = \sqrt{\frac{R_0 (n-q)(v+w)}{R_0 + (n-q)(v+w)}}\Big) \exp[-jk(n-q)(v+w)] \Big] \\ & + \sum_{r=1}^{n} E(r) \Big[\frac{R_0}{R'_{2(n-r)+1}} \exp[-jk(R_{2n} - R_{2r-1})] + \sqrt{\frac{R_0}{[(n-r)(v+w)+w][R_0 + (n-r)(v+w)+w]}} \\ & \cdot D\Big(\phi' = \alpha, \phi = \pi, L = \sqrt{\frac{R_0[(n-r)(v+w)+w]}{R_0 + [(n-r)(v+w)+w]}}\Big) \exp(-jk[(n-r)(v+w)+w]) \Big] \Big\} \end{aligned} \tag{11}$$

$$R_x = \begin{cases} \sqrt{\left[d + \frac{x}{2}(v+w)\right]^2 + H^2}, & x \quad even \\ \sqrt{\left[d + \frac{x-1}{2}(v+w) + v\right]^2 + H^2}, & x \quad odd \end{cases} \tag{12}$$

$$R'_x = \sqrt{\left[d + \frac{x-1}{2}(v+w) + w\right]^2 + H^2} \tag{13}$$

Expressing E_0 as in (3), D(ϕ, ϕ', L) represents the UTD diffraction coefficient for a finitely conducting wedge, as shown in [20], and $E(n)$ represents the field reaching the corners at the rooftops' right, as may be seen in Figure 1 (bottom):

$$\begin{aligned} E(n) = \frac{1}{2n-1}\Bigg\{ & E_0 A\left[\frac{R_0}{R_{2n-1}}\exp[-jk(R_{2n-1}-R_0)]\exp(-j\Delta k\Delta d\cos\alpha)\right. \\ & + \sqrt{\frac{R_0}{[n(v+w)-w][R_0+n(v+w)-w]}}\exp(-j\Delta k\Delta d) \\ & \left.\cdot D\left(\phi'=\frac{\pi}{2}+\alpha, \phi=\frac{3\pi}{2}, L=\sqrt{\frac{R_0[n(v+w)-w]}{R_0+[n(v+w)-w]}}\right)\cdot\exp(-jk[n(v+w)-w])\right] \\ & + \sum_{m=1}^{n-1} E_m\left[\frac{R_0}{R_{2(n-m)-1}}\exp[-jk(R_{2n-1}-R_{2m})]\right. \\ & + \sqrt{\frac{R_0}{[(n-m)(v+w)-w][R_0+(n-m)(v+w)-w]}} \\ & \left.\cdot D\left(\phi'=\frac{\pi}{2}+\alpha, \phi=\frac{3\pi}{2}, L=\sqrt{\frac{R_0[(n-m)(v+w)-w]}{R_0+[(n-m)(v+w)-w]}}\right)\cdot\exp(-jk[(n-m)(v+w)-w])\right] \\ & + \sum_{p=1}^{n-1} E(p)\left[\frac{R_0}{R_{2(n-p)}}\exp[-jk(R_{2n-1}-R_{2p-1})] + \sqrt{\frac{R_0}{(n-p)(v+w)[R_0+(n-p)(v+w)]}}\right. \\ & \left.\left.\cdot D\left(\phi'=\alpha, \phi=\pi, L=\sqrt{\frac{R_0(n-p)(v+w)}{R_0+(n-p)(v+w)}}\right)\cdot\exp(-jk(n-p)(v+w))\right]\right\} \end{aligned} \tag{14}$$

assuming the rest of the parameters defined as in the previous sub-section.

4. Measurement Setup

Figure 2 illustrates an outline of the measurement setup considered. This is an identical measurement set up to be carried out in [21–23]; however, in this instance, we assume the use of arrays of bonsai trees and bricks.

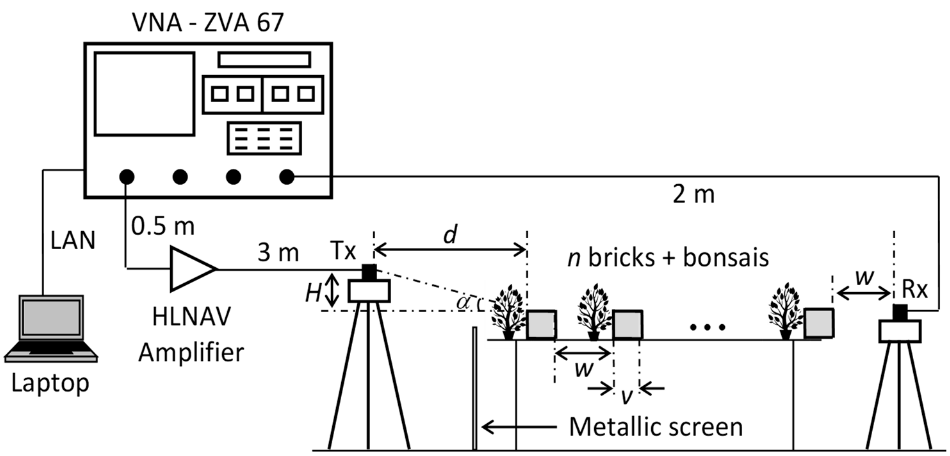

Figure 2. Scheme of the measurement setup.

A 38 to 40 GHz frequency band was considered. The assumed values were n = 1–3–5, w = 69.9 cm (90.9 λ), d = 1 m (130 λ) and hard/vertical polarization.

The width of the bricks was v = 5.1 cm; the five bonsai trees under consideration had a canopy with an average width of 20.8 cm (27 λ) and an average height of 14.6 cm (19 λ); the average leaf width was 2.3 cm (3 λ). We varied the height H of the transmitting antenna between 0 m and 0.04 m (5.2 λ)—implying that the bonsai canopy would always obstruct the direct ray (as occurs with the diffracted rays)—in increments of 0.01 m (1.3 λ) (five positions), which gave us the attenuation relative to the strength of the free-space field for all H values. Thus, the maximum value of the incident angle α was 2.29°, which is suitable for consideration of multiple-diffraction scenarios. We analyzed the channel frequency response using 293 frequency points, spaced at regular intervals across the 38–40 GHz range. Consequently, time aliasing was not present when measuring a maximum distance of 293/BW* 3 × 10^8 = 44 m; in this regard, it should be noted that the maximum dimension of the measurement environment was 7 m.

The antennas employed for measuring purposes were STEATITE Q-par 0.8 to 40 GHz omni-directional antennas [24] with a gain range between −2.2 and 6.9 dBi. Notably, this study assumes a far-field characterization. The maximum dimension of the antennas is D < 6 cm, and thus the far-field starts at 2D2/λ [25,26], that is, a distance of 0.93 m. As noted above, this paper considers the distance between the transmitter-first brick/bonsai pair to be 1 m. The used Rohde and Swartz ZVA 10 MHz–67 GHz Vector Network Analyzer (VNA) [27] had a power transmission of −20 dBm and an intermediate frequency of 1000 Hz. In addition, we correctly applied the time-gating technique presented in [21], allowing the selection of multiple-diffraction contributions to estimate relative attenuation while also eliminating any prevailing undesirable contributions.

5. Results

Figure 3 shows the attenuation at the Rx of Figure 2, relative to the free space field, as a function of H, obtained using the proposed UTD-PO formulation for trees and rectangular sections that undergoes comparison with the measurements from the scaled-model consisting of bonsai trees and bricks.

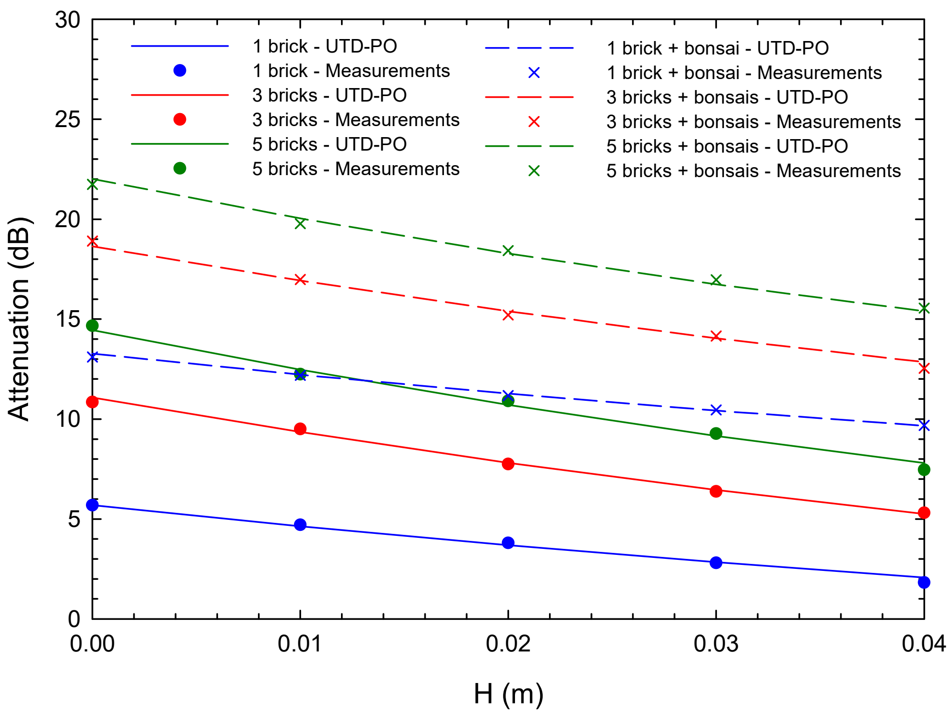

Figure 3. Comparison of the attenuation obtained with the UTD-PO solutions for rectangular sections (with and without trees), as a function of H, and measurements. Parameters of f = 39 GHz, n = 1–3–5, d = 1 m, w = 69.9 cm, v = 5.1 cm, relative permittivity of the bricks ε_r = 4.37 + 0.04j, Δd = 9 cm, hard/vertical polarization, and the COST 235 foliage-attenuation model for the in-leaf case have been considered.

For comparison, the outcomes of considering just rectangular sections (bricks) are also shown. In this case, the measurements were undertaken with no bonsai trees present and, for the theoretical predictions, the UTD-PO solution proposed by some of the authors of this research in [16] have been used. Parameters of f = 39 GHz, n = 1–3–5, d = 1 m, w = 69.9 cm, v = 5.1 cm, relative permittivity of the bricks ε_r = 4.37 + 0.04j [28], Δd = 9 cm, hard/vertical polarization, and the COST 235 foliage-attenuation model for the in-leaf case, have been considered. It should be noted that, with such parameters considered for the scaled-model, for example, in a real environment, a distance of 30 m between each tree-building pair would correspond to a frequency of 975 MHz. On the other hand, a step of 0.01 m has been assumed for the experimental data; therefore, considering the frequency employed (39 GHz), it leads to almost one measurement per wavelength, which is sufficient to ensure the accuracy of the results. As can be seen, there is a robust agreement between the measurements and the formulations from theory whether or not trees are present for the triple values of n under consideration. In relation to this, a significant offset of approximately 7.6 dB may be seen for formulations that incorporate trees and those which do not. Moreover, as H increases, the attenuation decreases in both cases owing to the less impact that multiple-building diffraction losses have at greater angles of incidence.

In Figure 4, the attenuation—relative to the free space field—obtained at the reference points of Figure 1 (middle and bottom) with the UTD-PO solutions proposed in this work for buildings modeled as knife-edges and rectangular sections, respectively, as a function of the number of obstacles, is depicted.

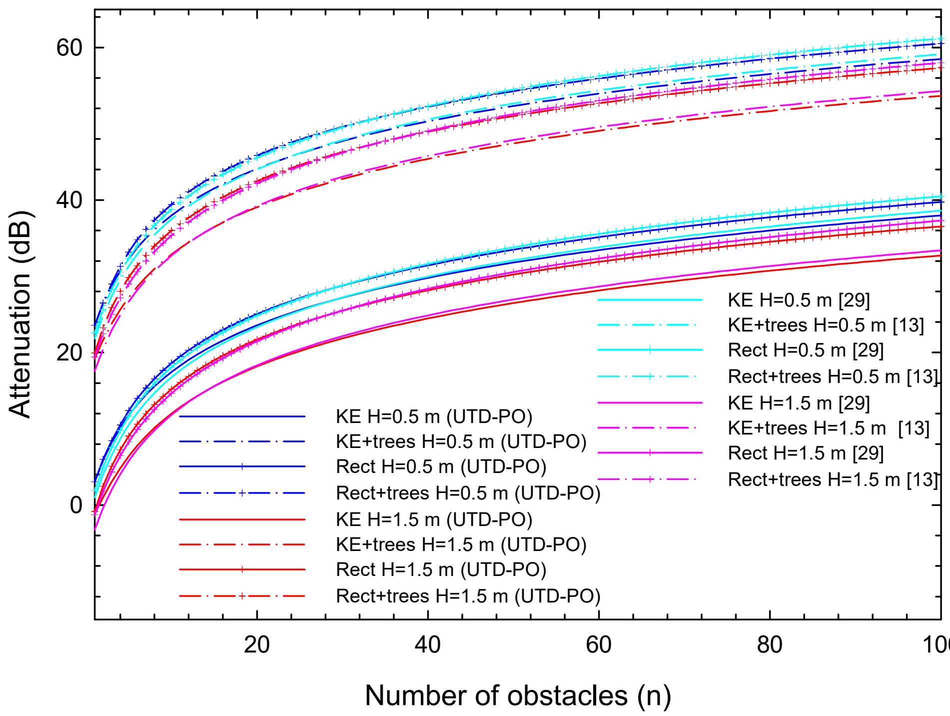

Figure 4. Attenuation obtained with the UTD-PO solutions (with and without trees) for buildings modeled as knife-edges and rectangular sections, as a function of the number of obstacles. Results obtained with models derived from [13,29] are also shown in the plot. Parameters of f = 3.5 GHz, d = 30 m, z = 50 m, w = 20 m, v = 30 m, relative permittivity of the bricks ε_r = 4 + 0.28j, Δd = 4 m, hard/vertical polarization, and the COST 235 foliage-attenuation model for the in-leaf case have been considered.

The figure also illustrates the outcomes when trees are absent and, in this instance, for the models considering buildings as knife-edges and rectangular shapes, we have taken into consideration the UTD-PO formulations proposed by some of the authors of this research in [16]. On the other hand, for comparison purposes, results obtained with models derived from [13,29] for multiple diffraction by buildings in the presence (and absence) of trees (when assuming spherical-wave incidence in both cases) are also shown in the plot. Parameters of 5G frequency f = 3.5 GHz, z = 50 m, $\underline{v}$ = 30 m, w = 20 m, relative permittivity of the bricks ε_r = 4 + 0.28j [30], Δd = 4 m, hard/vertical polarization, and the COST 235 foliage-attenuation model for the in-leaf case have been considered.

As can be observed, a solid agreement is obtained between the UTD-PO solutions proposed in this work and the methods derived from [13,29].

Furthermore, the influence of including trees as far as a diminution of the received field goes is extremely significant. This extra attenuation, which appears to reach a constant offset as n increases, can achieve a value, regarding the UTD-PO solutions, in the worst cases—H = 1.5 m (knife edges) and H = 0.5 m (rectangles)—of 20.93 and 20.78 dB, respectively.

On the other hand, building modeling appears to have a significant role too, being especially relevant when we assume higher angles of incidence (H = 1.5 m), causing extra attenuation (that, again, appears to settle with an increase in the quantity of obstacles) rising in the worst case scenario (H = 1.5 m) to 3.66 dB (when considering the UTD-PO formulations) for rectangular buildings plus trees rather than knife-edge buildings plus trees.

Finally, as was previously mentioned, attenuation values are greater—for both building modeling—with H = 0.5 m as compared to those obtained for H = 1.5 m, owing to the greater impact that the multiple-building diffraction phenomenon has at smaller angles of incidence in terms of signal losses.

6. Conclusions

This research has proposed a pair of UTD-PO formulations to calculate the multiple diffraction attenuation of radio waves caused by buildings and trees in vegetated urban areas. These solutions both make assumptions of spherical-wave incidence and consider buildings modeled as knife edges and rectangles (the latter being more complex and closer to reality), respectively. Proper validation of these formulations has been undertaken by comparing their attenuation predictions with other methods and measurements performed at 39 GHz with a scaled-model of the environment in question, built of bonsai trees and bricks. The chief advantage of these presented models is that, because of recursion, the calculations only require single diffractions, thus avoiding the need for higher-order diffraction terms for the diffraction coefficients, allowing for a lowering of the amount of computer time/power required.

The outcomes demonstrate that in both of the proposed formulations, it is clear that the existence of trees causes notable attenuation (up to almost 21 dB of additional losses at 3.5 GHz). Furthermore, the consideration of buildings modeled with greater realism (i.e., rectangular sections) supposes extra losses that would not have arisen with less complex knife-edge modeling. The outcomes of this research may be used when planning future mobile communication systems, including 6G networks and beyond.

Author Contributions: Conceptualization, J.-V.R. and L.J.-L.; methodology, J.-V.R., M.-T.M.-I., J.-M.M.G.-P., L.J.-L. and I.R.-R.; software, J.-V.R. and L.J.-L.; validation, J.-V.R., M.-T.M.-I., J.-M.M.G.-P., L.J.-L. and I.R.-R.; formal analysis, J.-V.R., M.-T.M.-I., J.-M.M.G.-P., L.J.-L. and I.R.-R.; investigation, J.-V.R., M.-T.M.-I., J.-M.M.G.-P., L.J.-L. and I.R.-R.; resources, J.-V.R., M.-T.M.-I., J.-M.M.G.-P., L.J.-L. and I.R.-R.; data curation, J.-V.R., M.-T.M.-I., J.-M.M.G.-P., L.J.-L. and I.R.-R.; writing—original draft preparation, J.-V.R.; writing—review and editing, J.-V.R., M.-T.M.-I., J.-M.M.G.-P., L.J.-L. and I.R.-R.; visualization, J.-V.R., M.-T.M.-I., J.-M.M.G.-P., L.J.-L. and I.R.-R.; supervision, J.-V.R., M.-T.M.-I., J.-M.M.G.-P., L.J.-L. and I.R.-R.; project administration, J.-M.M.G.-P. and L.J.-L.; funding acquisition, J.-M.M.G.-P. and L.J.-L. All authors have read and agreed to the published version of the manuscript.

Funding: This work was supported by the Ministerio de Ciencia e Innovación, Spain under Grant PID2019-107885GB-C33.

Institutional Review Board Statement: Not applicable.

Informed Consent Statement: Not applicable.

Data Availability Statement: The data that support the findings of this study are available on request from the corresponding author.

Conflicts of Interest: The authors declare no conflict of interest.

References

1. Walfisch, J.; Bertoni, H. A theoretical model of UHF propagation in urban environments. *IEEE Trans. Antennas Propag.* **1988**, *36*, 1788–1796. [CrossRef]
2. Xia, H.; Bertoni, H. Diffraction of cylindrical and plane waves by an array of absorbing half-screens. *IEEE Trans. Antennas Propag.* **1992**, *40*, 170–177. [CrossRef]
3. Saunders, S.R.; Bonar, F.R. Explicit Multiple Building Diffraction Attenuation Function for Mobile Radio Wave Propagation. *Electron. Lett.* **1991**, *27*, 1276–1277. [CrossRef]
4. Holm, P. UTD-diffraction coefficients for higher order wedge diffracted fields. *IEEE Trans. Antennas Propag.* **1996**, *44*, 879–888. [CrossRef]
5. Neve, M.J.; Rowe, G.B. Contributions towards the Development of a UTD-Based model for Cellular Radio Propagation Prediction. *IEE Proc. Microw. Ant. Prop.* **1994**, *141*, 407–414. [CrossRef]
6. Volkova, A.; Malevich, E.; Mikhailov, M. Numerical Simulation of Radio Wave Propagation in a Forest Environment Using the Constructor of Individual Trees. In Proceedings of the 2019 Radiation and Scattering of Electromagnetic Waves (RSEMW), Divnomorskoe, Russia, 24–28 June 2019; pp. 360–363. [CrossRef]
7. Picallo, I.; Klaina, H.; Lopez-Iturri, P.; Aguirre, E.; Celaya-Echarri, M.; Azpilicueta, L.; Eguizábal, A.; Falcone, F.; Alejos, A. A Radio Channel Model for D2D Communications Blocked by Single Trees in Forest Environments. *Sensors* **2019**, *19*, 4606. [CrossRef]
8. Adegoke, A.S.; Okpeki, U.K.; Green, O. Radio Wave Propagation in a Forested Channel. *J. Eng. Res. Rep.* **2022**, *22*, 34–40. [CrossRef]
9. Segun, A.A.; Kofoworola, A.H.; Chizea, F.D.; Gbenro, A.; Benjamin AS, A. Scattering Effects of Residential Trees on Very High Frequency Radio Wave Propagation. *Adv. Phys. Theor. Appl.* **2020**, *83*, 76–86.
10. Adegoke, A.S.; Okpeki, U.K.; Green, O. Path Loss Prediction Model for Propagating Radio Wave in Woodland. *J. Eng. Res. Rep.* **2022**, *22*, 1–9. [CrossRef]
11. Torrico, S.; Bertoni, H.; Lang, R. Modeling tree effects on path loss in a residential environment. *IEEE Trans. Antennas Propag.* **1998**, *46*, 872–880. [CrossRef]
12. Chee, K.L.; Torrico, S.A.; Kurner, T. Radiowave Propagation Prediction in Vegetated Residential Environments. *IEEE Trans. Veh. Technol.* **2012**, *62*, 486–499. [CrossRef]
13. Ghorbani, A.; Tajvidy, A.; Torabi, E.; Arablouei, R. A New Uniform Theory of Diffraction Based Model for Multiple Building Diffraction in the Presence of Trees. *Electromagnetics* **2011**, *31*, 127–146. [CrossRef]
14. Zhang, W. Formulation of multiple diffraction by trees and buildings for radio propagation predictions for local multipoint distribution service. *J. Res. Natl. Inst. Stand. Technol.* **1999**, *104*, 579–584. [CrossRef]
15. Erricolo, D.; D'Elia, G.; Uslenghi, P. Measurements on scaled models of urban environments and comparisons with ray-tracing propagation simulation. *IEEE Trans. Antennas Propag.* **2002**, *50*, 727–735. [CrossRef]
16. Rodríguez, J.-V.; Molina-García-Pardo, J.-M.; Juan-Llácer, L. A new solution expressed in terms of UTD coefficients for the multiple diffraction of spherical waves by a series of buildings. *Radio Sci.* **2007**, *42*, 1–15. [CrossRef]
17. Kouyoumjian, R.; Pathak, P. A uniform geometrical theory of diffraction for an edge in a perfectly conducting surface. *Proc. IEEE* **1974**, *62*, 1448–1461. [CrossRef]
18. *COST235: Radio Propagation Effects on Next-Generation Fixed-Service Terrestrial Telecommunication Systems*; Final Report; CCLRC Rutherford Appleton Laboratory (RAL): Luxembourg, 1996.
19. Matzler, C. Microwave (1-100 GHz) dielectric model of leaves. *IEEE Trans. Geosci. Remote Sens.* **1994**, *32*, 947–949. [CrossRef]
20. Luebbers, R. Finite conductivity uniform GTD versus knife edge diffraction in prediction of propagation path loss. *IEEE Trans. Antennas Propag.* **1984**, *32*, 70–76. [CrossRef]
21. Martinez-Ingles, M.-T.; Rodriguez, J.-V.; Molina-Garcia-Pardo, J.-M.; Pascual-Garcia, J.; Juan-Llacer, L. Comparison of a UTD-PO Formulation for Multiple-Plateau Diffraction With Measurements at 62 GHz. *IEEE Trans. Antennas Propag.* **2012**, *61*, 1000–1003. [CrossRef]
22. Martinez-Ingles, M.-T.; Rodriguez, J.-V.; Molina-Garcia-Pardo, J.-M.; Pascual-Garcia, J.; Juan-Llacer, L. Experimental and Theoretical Comparison of Cylindrical Against Rectangular Obstacles in mm-Wave Multiple Diffraction. *IEEE Trans. Antennas Propag.* **2013**, *61*, 5347–5350. [CrossRef]
23. Martinez-Ingles, M.-T.; Rodriguez, J.-V.; Pascual-Garcia, J.; Molina-Garcia-Pardo, J.-M.; Juan-Llacer, L. On the Influence of Diffuse Scattering on Multiple-Plateau Diffraction Analysis at mm-Wave Frequencies. *IEEE Trans. Antennas Propag.* **2019**, *67*, 2130–2135. [CrossRef]
24. Ultra-Wideband Omni-Directional Antenna 0.8 to 40 GHz. Available online: https://www.steatite-antennas.co.uk/wp-content/uploads/2017/09/QOM-SL-0.8-40-K-SG-L.pdf (accessed on 9 February 2023).
25. Balanis, C.A. *Antenna Theory: Analysis and Design*; Wiley: New York, NY, USA, 1997.
26. Rappaport, T.S. *Wireless Communications: Principles and Practice*; Prentice-Hall: Upper Saddle River, NJ, USA, 2002.
27. R&S®ZVA vector network analyzer. Available online: https://www.rohde-schwarz.com/es/producto/zva-pagina-de-inicio-producto_63493-9660.html (accessed on 9 February 2023).
28. Alejos, A.V.; Sanchez, M.G.; Cuinas, I. Measurement and Analysis of Propagation Mechanisms at 40 GHz: Viability of Site Shielding Forced by Obstacles. *IEEE Trans. Veh. Technol.* **2008**, *57*, 3369–3380. [CrossRef]

29. Tajvidy, A.; Ghorbani, A. A New Uniform Theory-of-Diffraction-Based Model for the Multiple Building Diffraction of Spherical Waves in Microcell Environments. *Electromagnetics* **2008**, *28*, 375–387. [CrossRef]
30. Muqaibel, A.; Safaai-Jazi, A.; Bayram, A.; Attiya, A.; Riad, S. Ultrawideband through-the-wall propagation. *IEE Proc.–Microw. Antennas Propag.* **2005**, *152*, 581–588. [CrossRef]